Thermal, Fluid, Mechanical, and Microstructural Property Characterization of Additively Manufactured Lattice Structures

Omar Mireles, Carlos Gomez, William Tilson, Travis Belcher, Brandon Abranovic, Mariana Chaidez, John Lopez, Christopher Romanowski, and Lief Wesche.

NASA Marshall Space Flight Center

Lattice Structure Applications

- Applications
  - Reduce weight, retain stiffness.
  - Variable relative density (%RD) & surface area.
  - Permeable solid: metal porous foam & Regimesh replacement.
  - Metal matrix composite (back infiltration).
  - Custom property potential: mimic properties of different materials in the same part using the same material in adjacent regions.

- Limitations
  - Computationally expensive.
  - Inadequate property data.


Green Propulsion Thruster Catalyst Bed

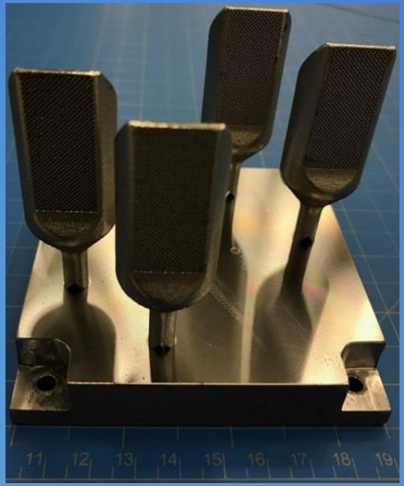
Propellant Management Device Demo


Lattice Regen Chamber Demo


ECLSS 4-Bed Molecular Sieve (4BMS-X) Heater Plate

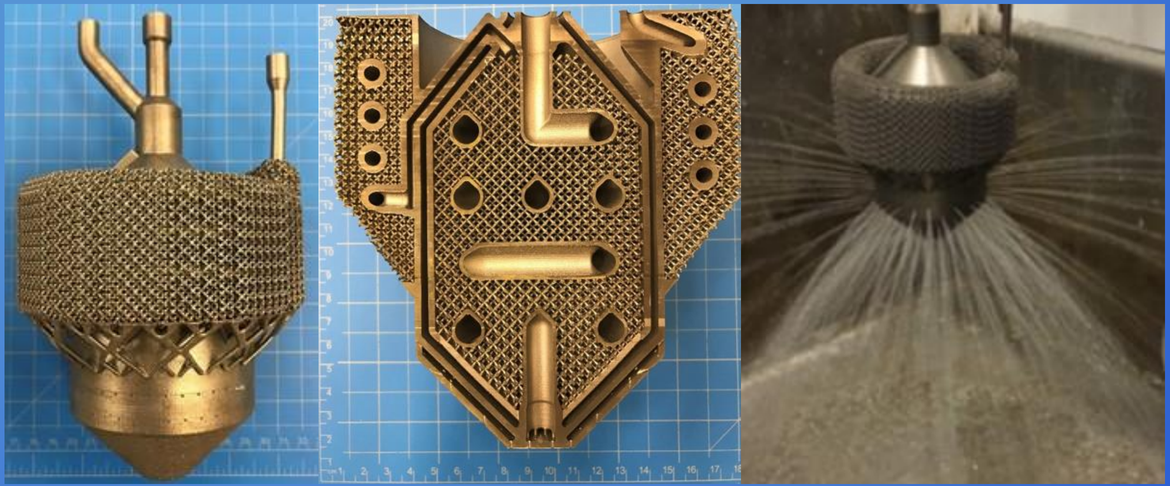
Cryo Heat Exchanger-Injector-Condenser Demonstrator


KSC O_2 Generator Cold-Head

Objectives

- Down-select lattice topology candidates
  - Evaluate computational expense
  - Evaluate SLM printability
- Investigate lattice structure engineering utility
  - Mechanical properties
  - Thermal properties
  - Flow properties
  - Microstructural characterization
- Evaluate for broad-scale performance trends
  - Topology
  - Unit cell (a) and strut thickness (t)
  - Material
  - Machine

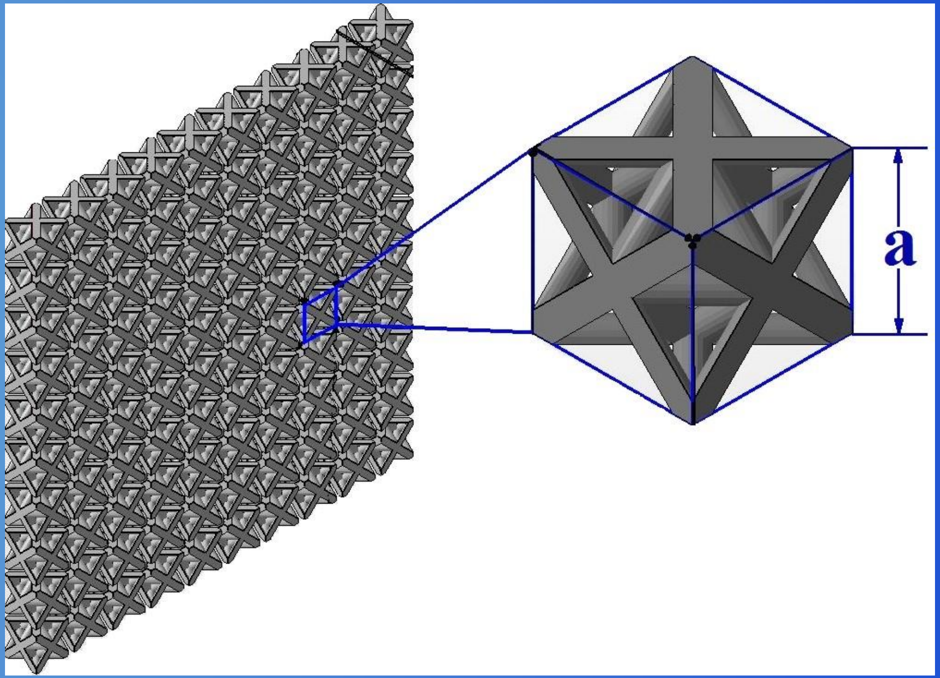

Lattice unit cell (a) and strut thickness (t).

Computational Expense

- Lattices topology generation
  - Materialise Magics structures module
- Standardized volume
  - 10x10x10 mm cube
- Unit Cell Sizes
  - 1 mm & 10 mm
  - Strut dependent on unit cell
- Established selection criteria
  - Processing time
  - File size
  - SLM printability

No	Name	Image	Unit Cell (mm)	Processing Time (s)	.stl Size (KB)	Used in Test Builds?	Successful Build?	Machine
1	Body diagonals with nodes rounded		10	1	144			
			1	300	56021			
2	Body diagonals with nodes		10	1	126			
			1	240	15,296			
3	Cross (10.4% relative density)	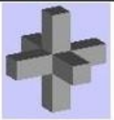	10	1	4	ASTM E8 - 0.5 mm	N - 90 deg unsupported surface	M290
			1	3	2442			
4	Cross-1		10	1	8		N - 90 deg unsupported surface	
			1	4	6350			
5	Cross-2		10	1	6		N - 90 deg unsupported surface	
			1	3	4788			
6	Cross-3		10	1	6		N - 90 deg unsupported surface	
			1	3	4006			
7	Cross-X		10	1	22			
			1	35	6131			
8	Cross-X _reeinforced		10	1	5		N - 90 deg unsupported surface	
			1	3	1911			
9	Diamond 20 percent relative density		10	5	384	Lattice Backfill 2, 4 mm	Y - All	M1, M290
			1	600	19331			

Example of lattice generation time and file size.

Metal Printability

- Down-Selected 4 lattice cell topologies
  - Diamond - 20%RD
  - Dode Medium - 13%RD
  - Octet Truss - 30%RD
  - Rhombic Dodecahedron - 20%RD
- Down-Selected 2 lattice unit cell sizes
  - Course: 5 mm
  - Fine: 2 mm
- Specimens produced on several platforms
  - EOS M290: IN718, stress relief, HIP, and solution/age per AMS 5664.
  - Concept Laser M1: IN625, annealed.
  - Concept Laser M2: GRCop84, as built.
  - Concept Laser X-Line 1000R: AlSi10Mg, as built at stress relief temp.
- Cross-Sectional Area Measurement
  - CAD
  - Specimen

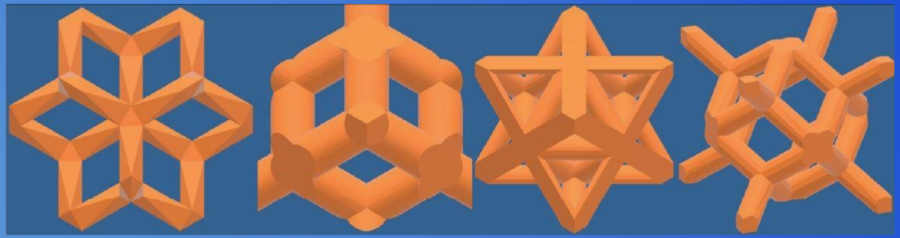

Dode Medium-13%RD | Diamond-20%RD | Octet Truss -30%RD | Rhombic Dodecahedron -20%RD

GRCop84 Met Cubes.
(L) a = 5 mm, (R) = 2 mm.

Mechanical Testing

- IN718 – fully heat treated
- Strength calculations based on assumed minimum cross sectional area from CAD.
- Displacement control rate: 0.508 mm/min.

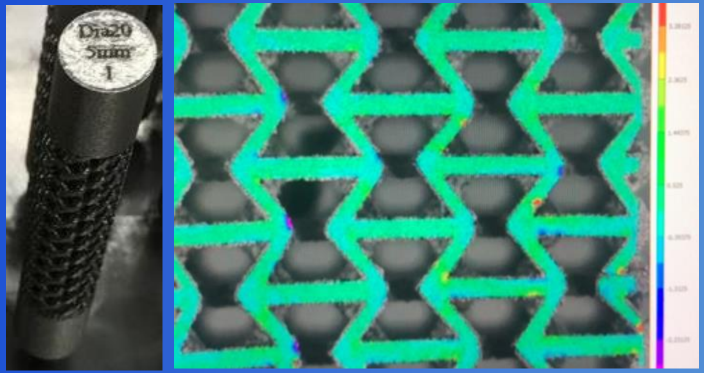

Lattice Compression Strain Field

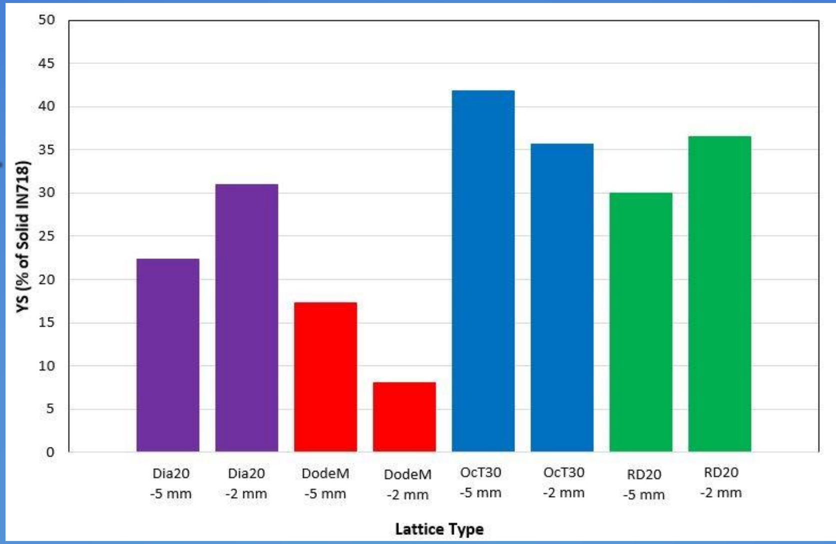

Effective Yield Strength of IN718 Lattice

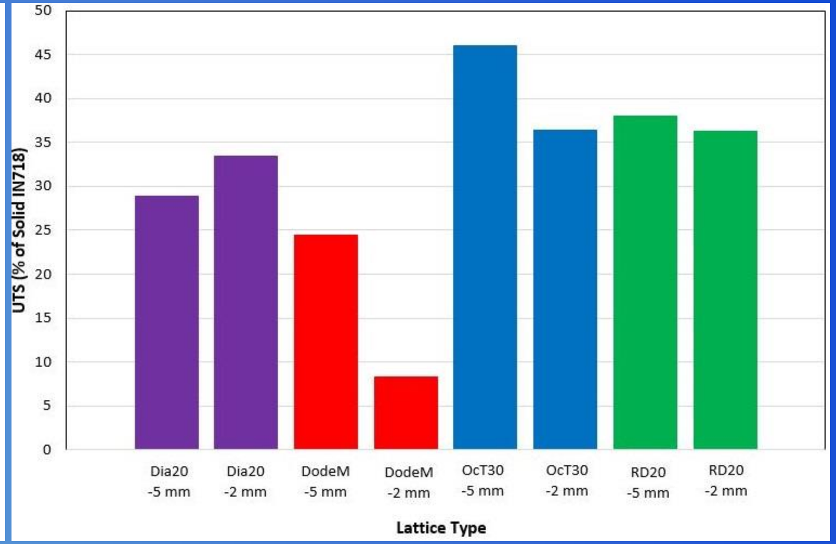

Effective Ultimate Strength of IN718 Lattice

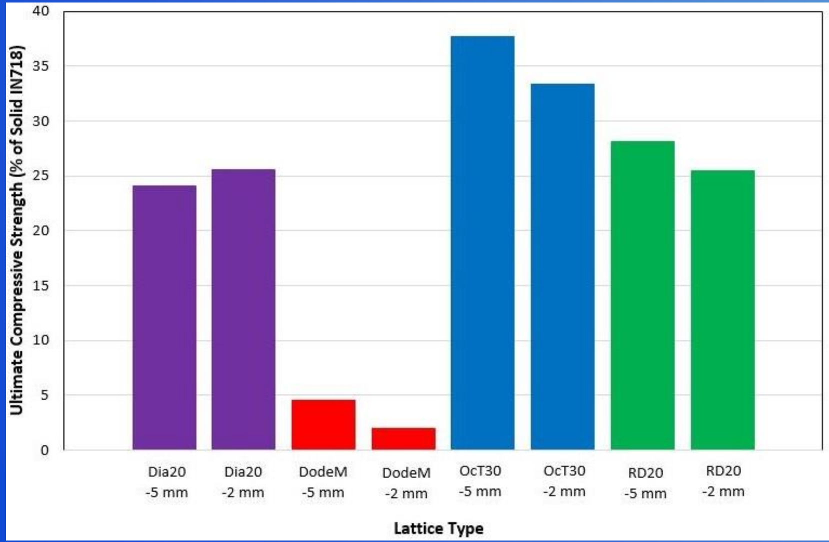

Effective Ultimate Compressive Strength of IN718 Lattice

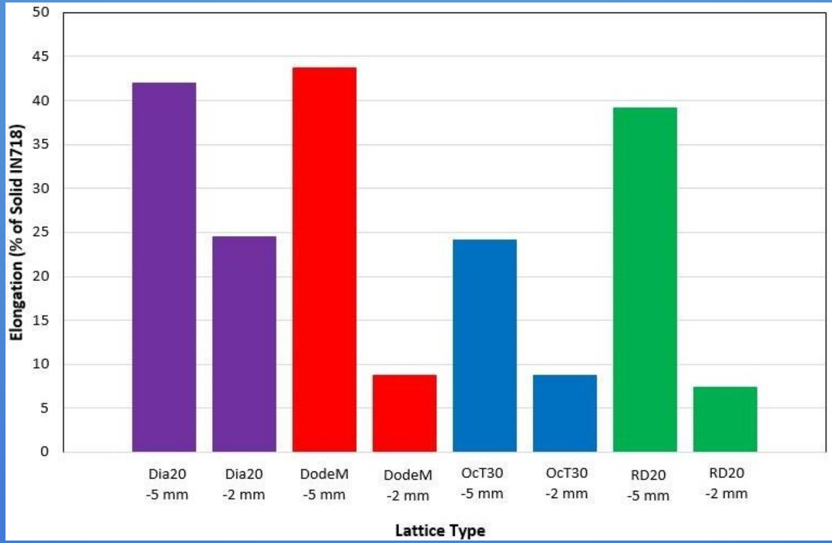

Effective Elongation of IN718 Lattice

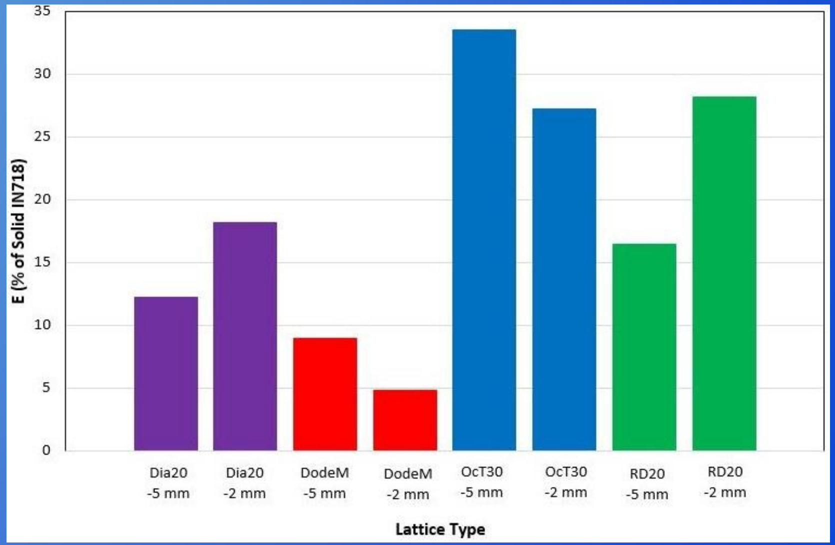

Effective Modulus of IN718 Lattice

Mechanical Testing

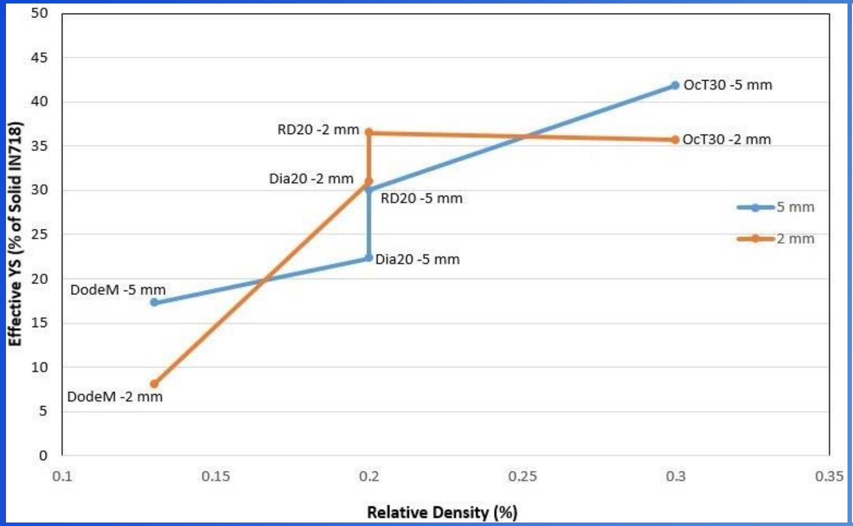

Effective Yield Strength vs. %RD

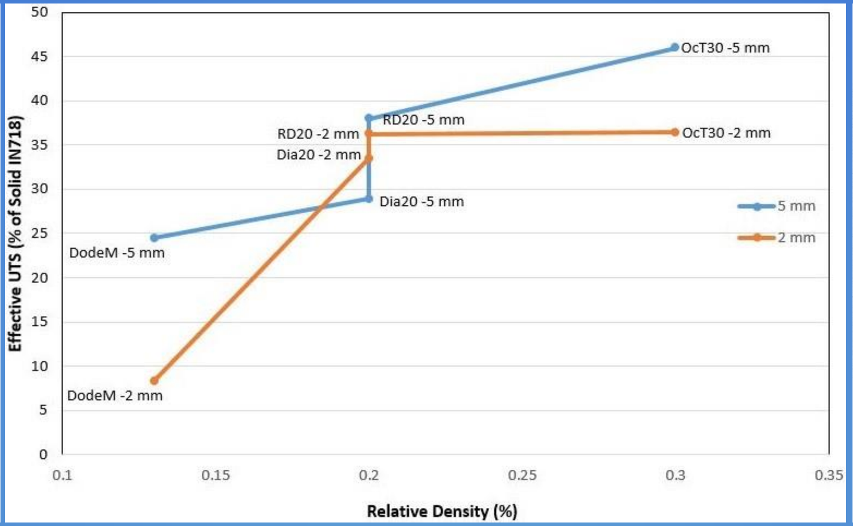

Effective Ultimate Strength vs. %RD

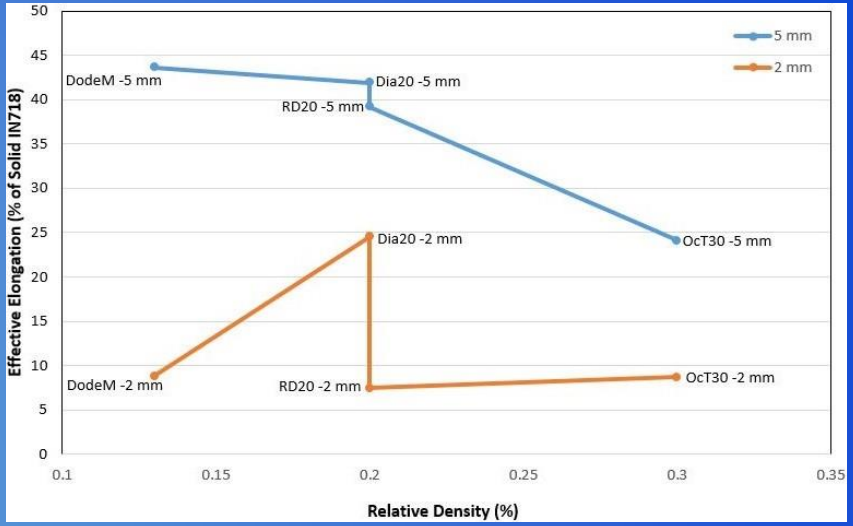

Effective Elongation vs. %RD

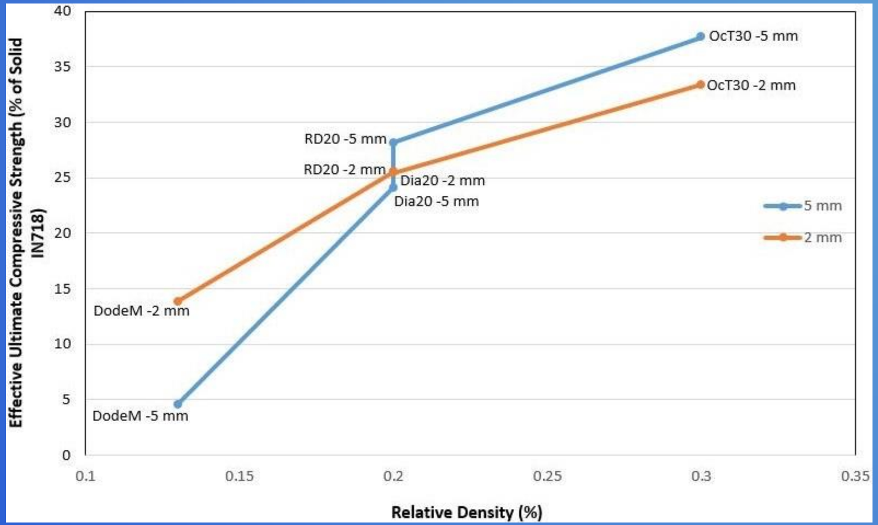

Effective Ultimate Compressive Strength vs. %RD

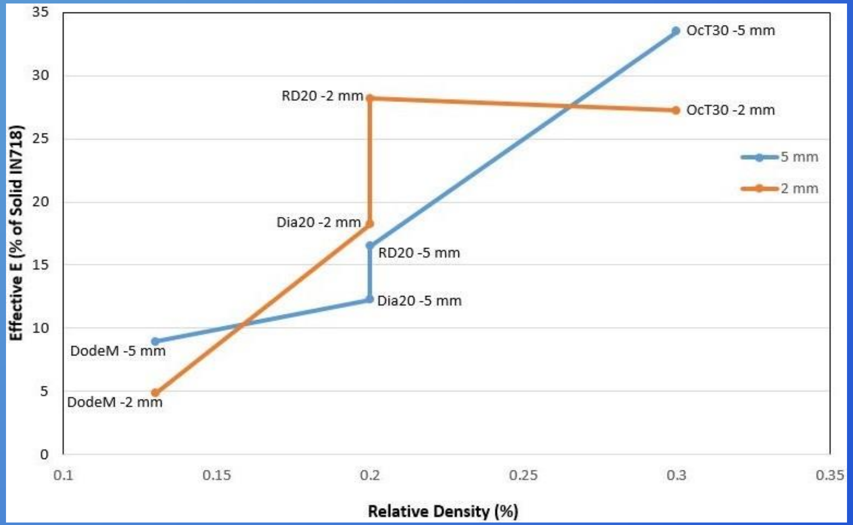

Effective Modulus vs. %RD

- Strong dependence on %TD followed by lattice topology and to a lesser extent unit cell size.

Fracture Surface Inspection

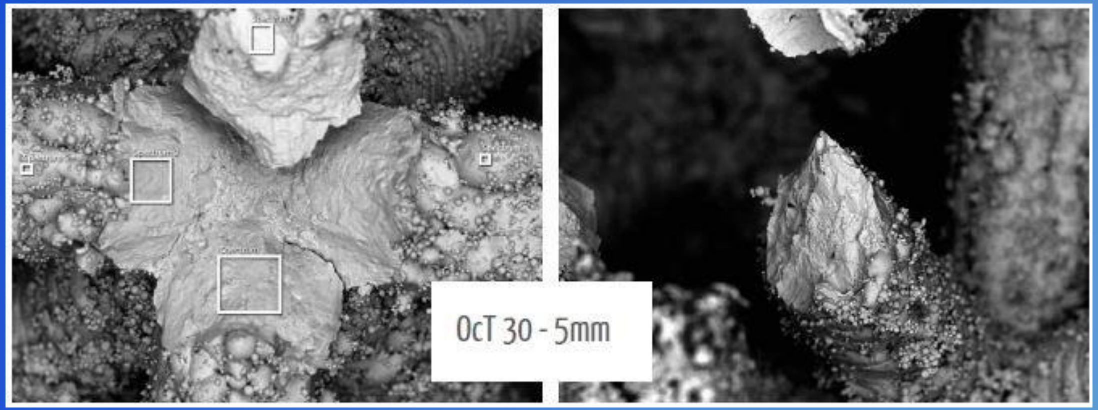

Fractures consistently occur at similar points within a unit cell.

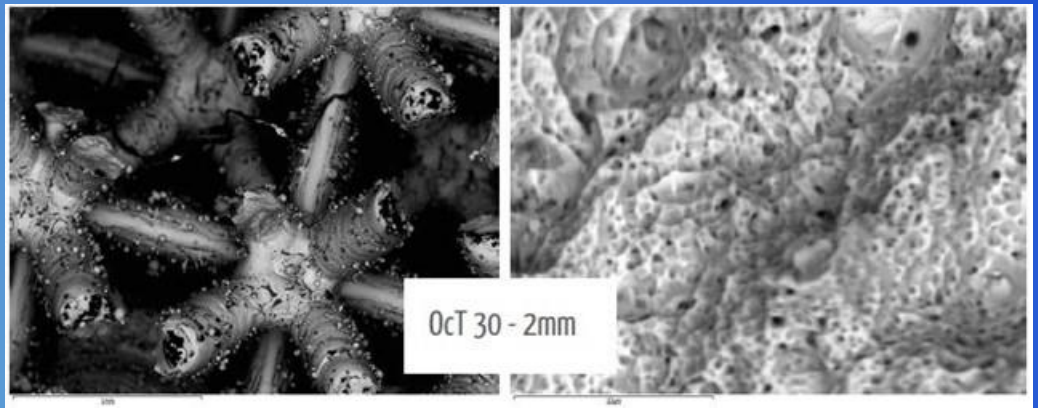

Dimple ductile fracture.

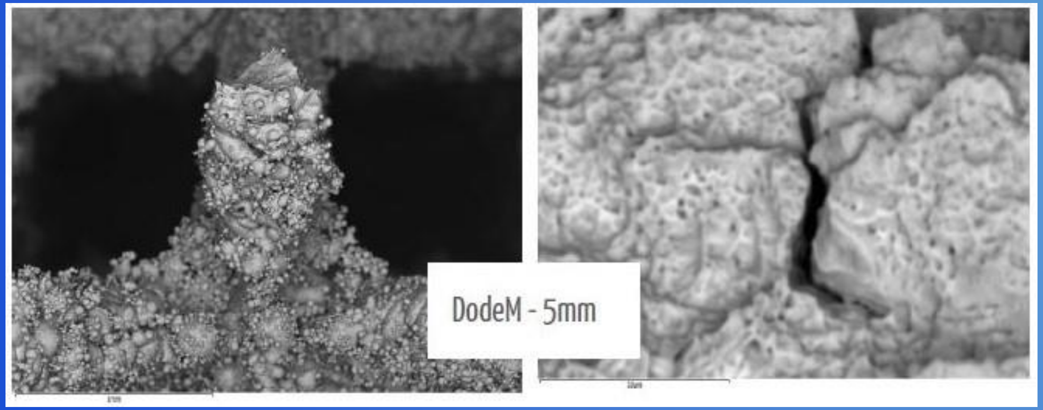

Prone to crack nucleation and low strain failure.

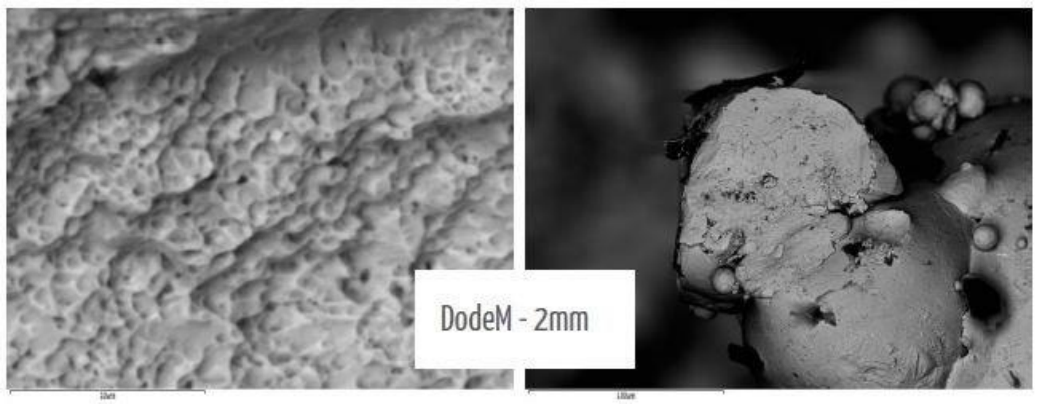

Ductile and brittle signatures at different regions on fracture.

Model Control Volume & Boundary Conditions

- Steady State.
- Aluminum properties assumed constant with temperature to simplify effective thermal conductivity calculations.
  - $K = 205$ W/m-K
  - $C_p = 0.9$ J/g-K
  - $\rho = 2700$ kg/m^3

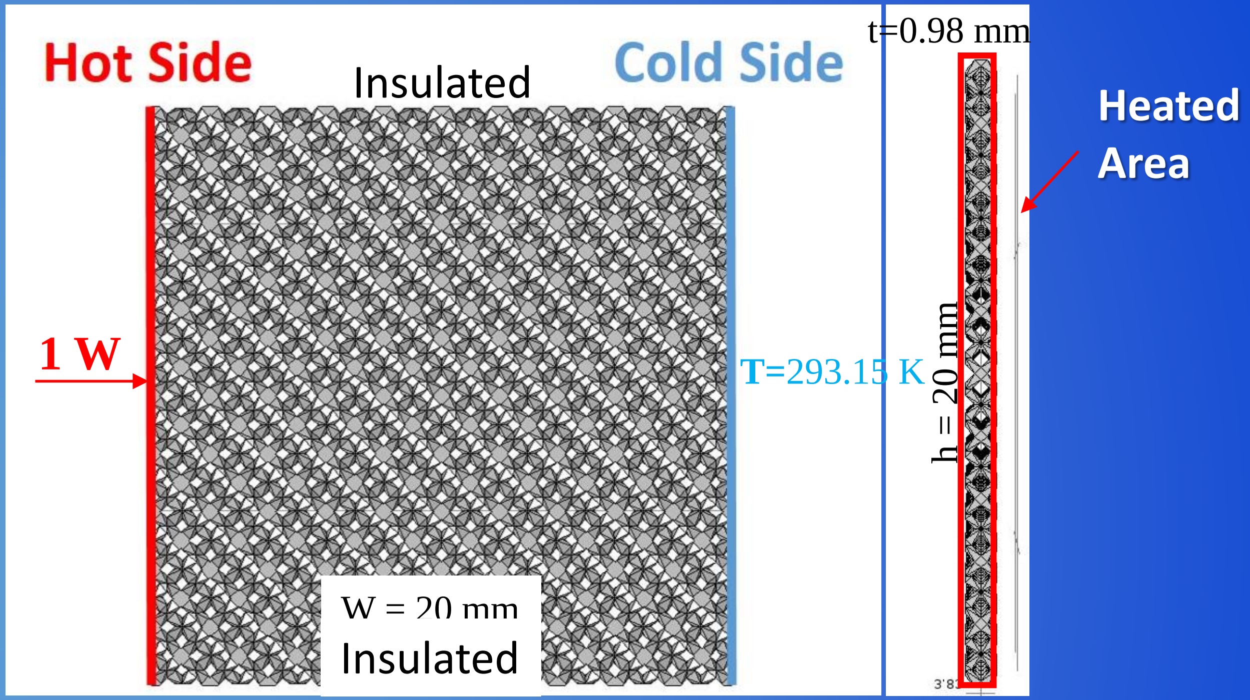

$$k = \frac{QL}{A\Delta T}$$

k - Thermal Conductivity

Q - Heat Flux

L - Length

A - Cross-Sectional Area

ΔT - Differential Temperature

$$\alpha = \frac{k_{eff}}{\rho_{eff} C_p}$$

α - Thermal Diffusivity

k_{eff} - Effective Thermal Conductivity

ρ_{eff} - Effective Density (M_{model}/V_{max})

C_p - Specific Heat Capacity

Simulation Results

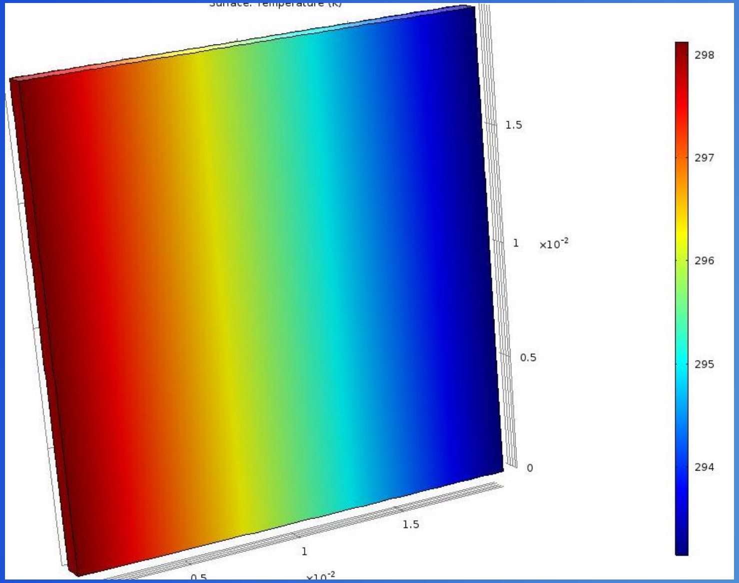

Solid Model

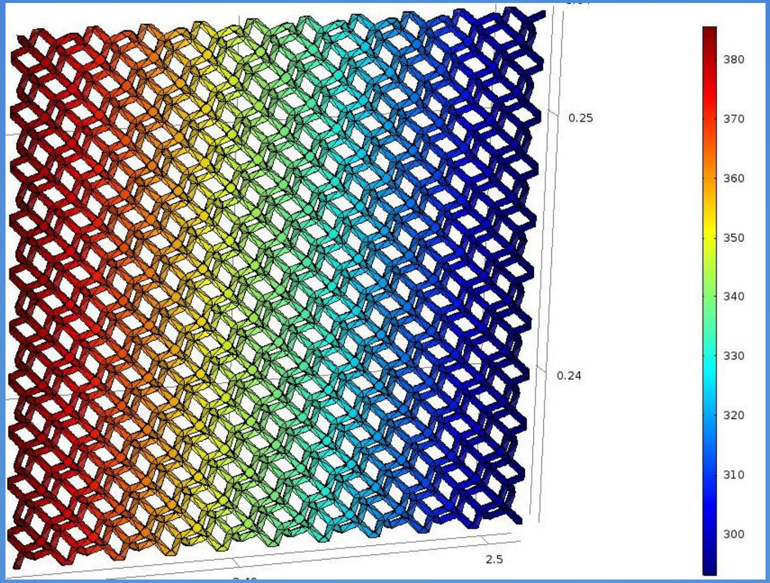

Medium Lattice Model

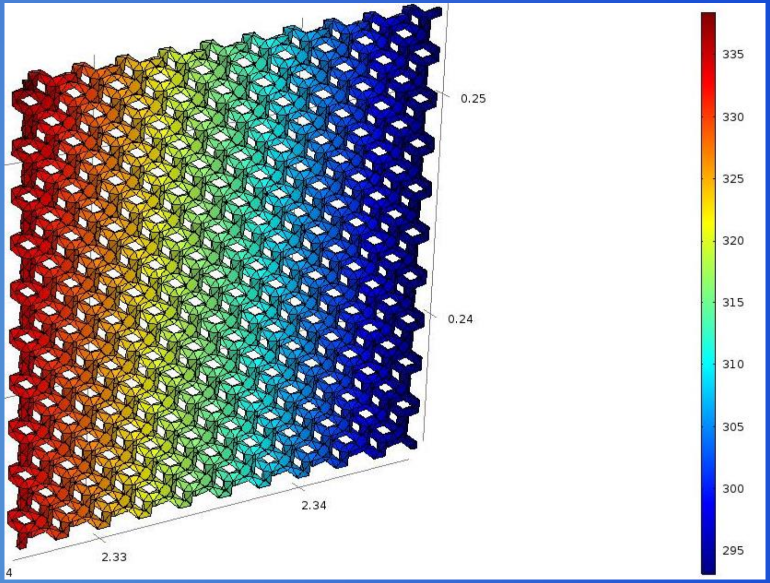

Thick Lattice Model

Model	Surf. Area (mm^2)	Volume (mm^3)	Mass (g)	ΔT (K)	k_{eff} (W/m-K)	α (mm^2/s)	Void Fraction
Solid	878.4	392.0	1.058	4.98	204.9	84.32	0.000
Medium Lattice	933.6	49.96	0.135	92.45	11.04	35.64	0.873
Thick Lattice	1240	97.54	0.263	45.27	22.54	37.28	0.751

$$Void\ Fraction = 1 - \rho_{rel}$$

Effective Thermal Conductivity vs. Void Fraction

- Effective thermal conductivity is inversely proportional to void fraction, which is lattice geometry specific.

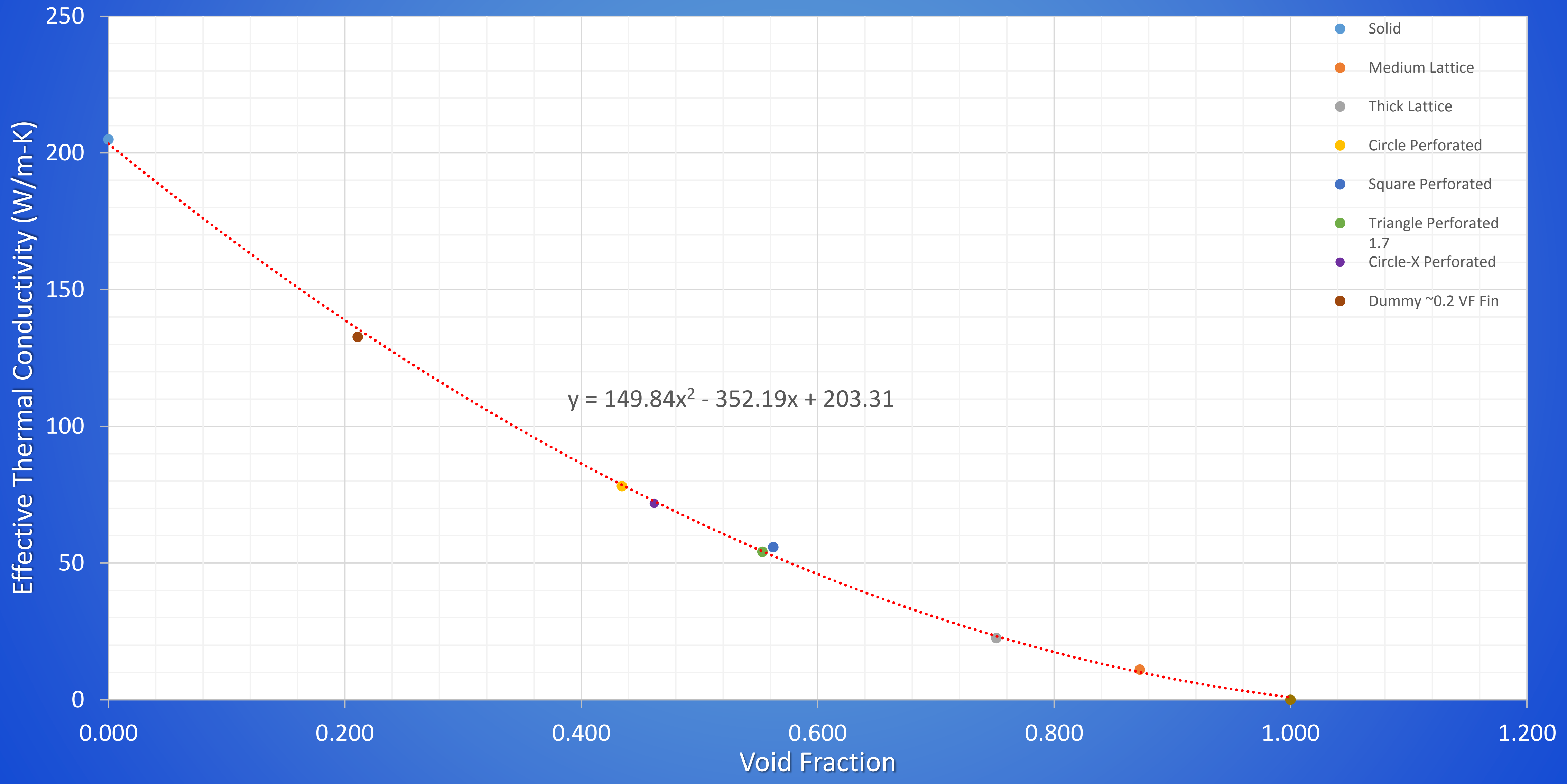

Thermal Conductivity

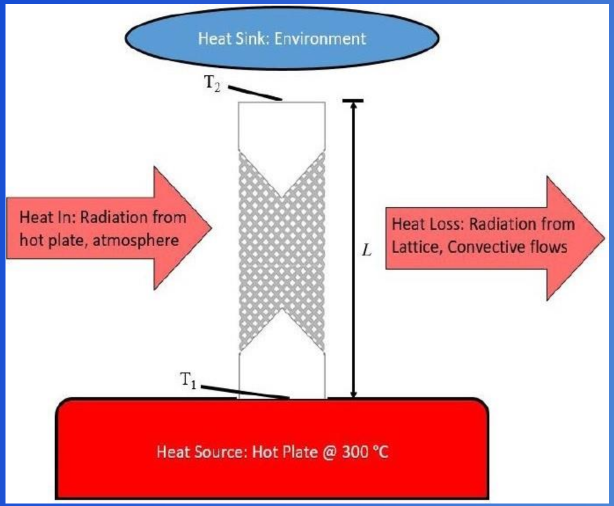

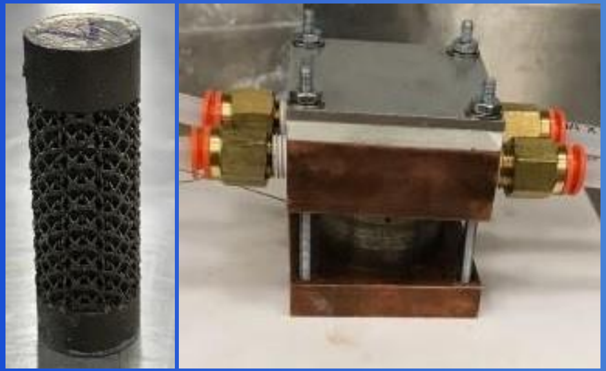

Thermal conductivity specimen and experimental test apparatus based on modified ASTM 1225-04.

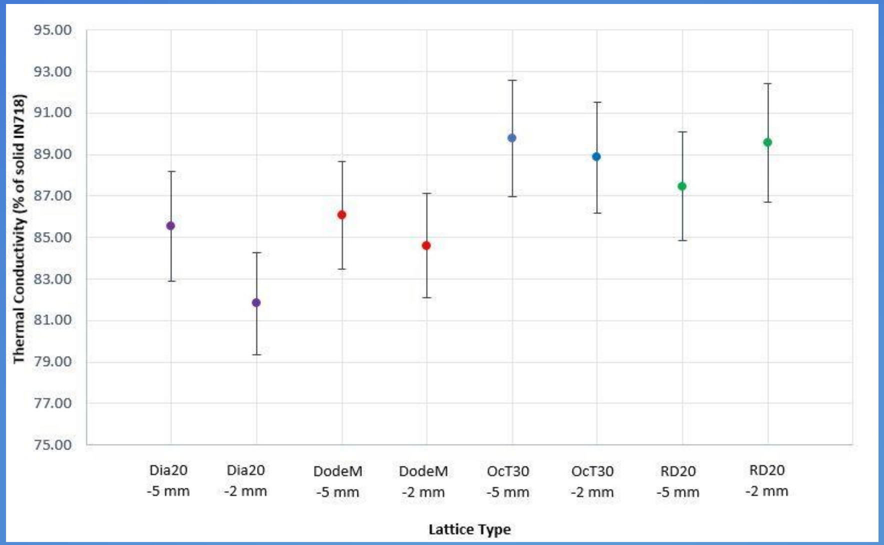

Thermal conductivity of IN718 lattices.

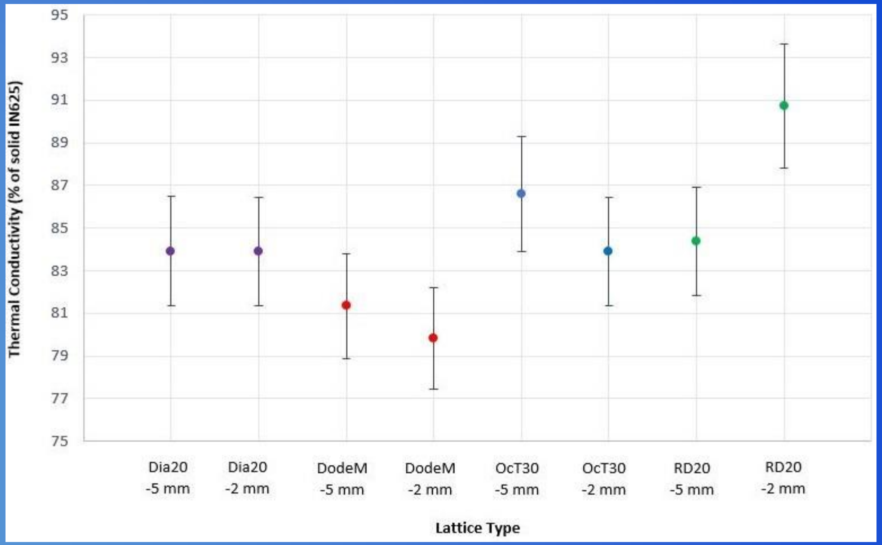

Thermal conductivity of IN625 lattices.

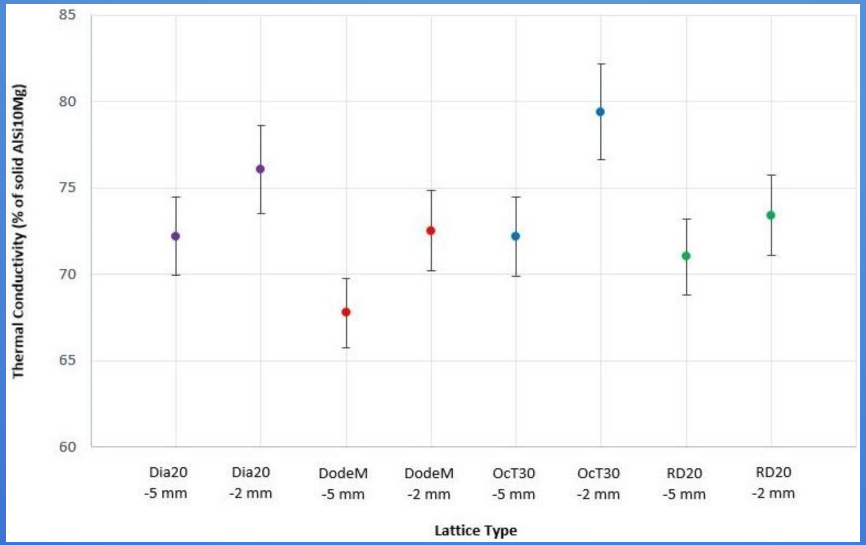

Thermal conductivity of AlSi10Mg lattices.

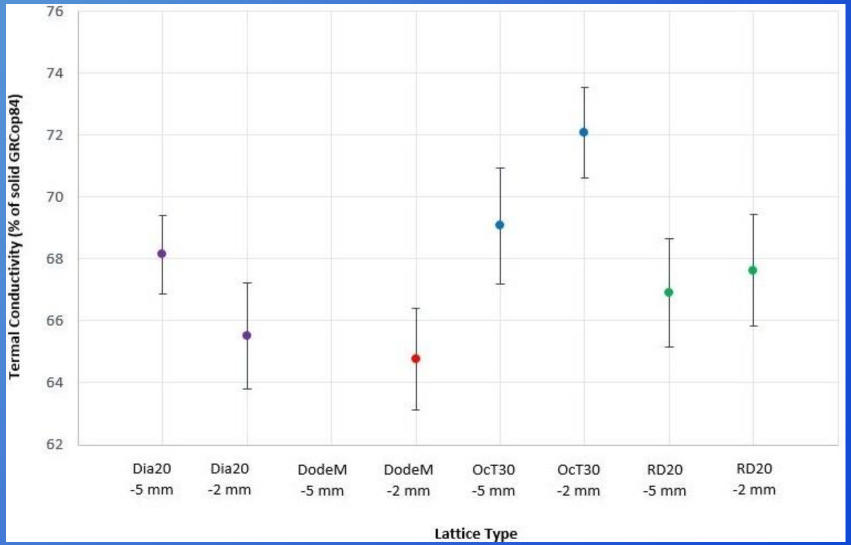

Thermal conductivity of GRCop84 lattices.

Flow & Convective Heat Transfer Coefficients

- Flow Coefficient (K_v)
  - Flow rate (m^3/hr) of water at 16 °C with a pressure drop across a valve of 1 bar.
  - $C_v = 1156 \cdot K_v$

- Convective Heat Transfer Coefficient (h)
  - Packed bed model
  - Order of magnitude difference between predicted and experimental results.

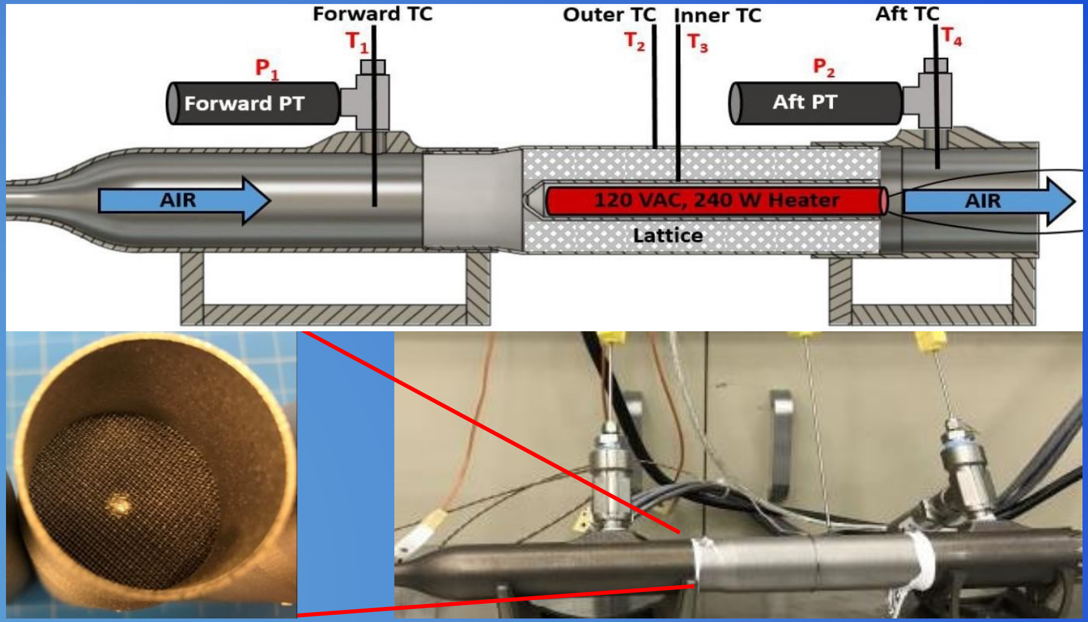

Annulus specimen & test apparatus.

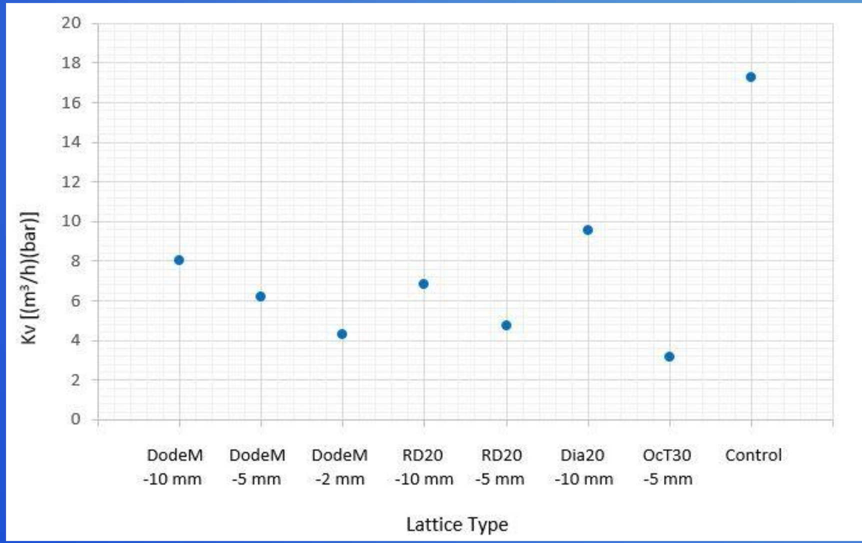

Flow coefficients of lattice types.

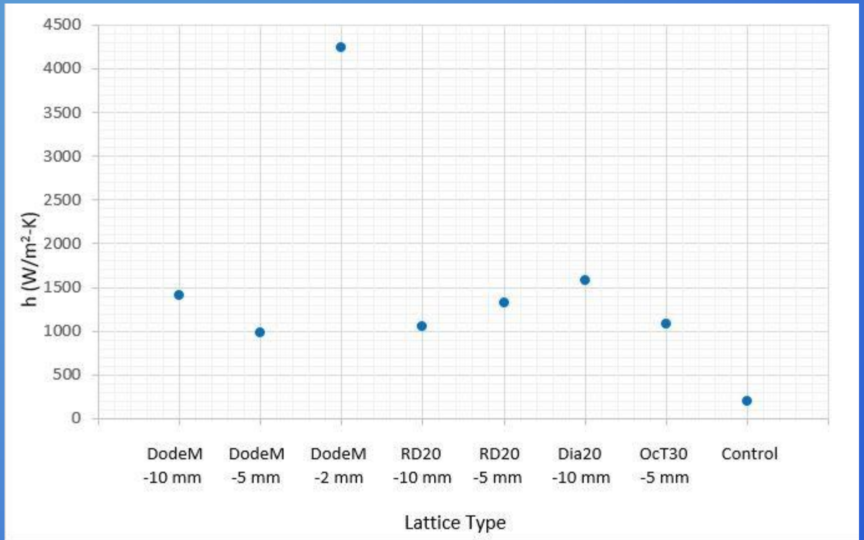

Convective heat transfer coefficient of lattice types.

Lattice Infiltration

- Low cost metal matrix composite (MMC)
  - High strength structure.
  - High thermal conductivity infill.
  - Functional transition gradient.

- IN718 lattice cube (10x10x10 mm) in mold cup
  - Specimens printed on the M290.
  - Vibratory fill with C18150 power.

- Infiltration
  - 1093 °C for 1 hr in argon to melt C18150.

- Infiltration Evaluation
  - Metallographic preparation.
  - Imaged using Canon EOS T6 camera and Keyence VHX-500 optical microscope at 100x.

Material	ρ (g/cm^3)	T_m (°C)	k (W/m-K)	Notes
IN718	8.22	1370-1430	6.5	AM cup & lattice cube
C18150 (CuCr1Zr)	8.89	1080	323.4	Backfill powder

Sample Number	Lattice Style	Unit Cell (mm)
1	Dode-Medium (13% relative density)	5.0
2		2.0
3	Rhombic Dodecahedron-20% relative density	5.0
4		2.0
5	Diamond-20% relative density	5.0
6		2.0
7	Octet Truss-30% relative density	5.0
8		2.0
9	Cross - 10.4% relative density	2

Vibratory Powder Fill Station

Back Infiltration Specimen Build

Infiltration Results

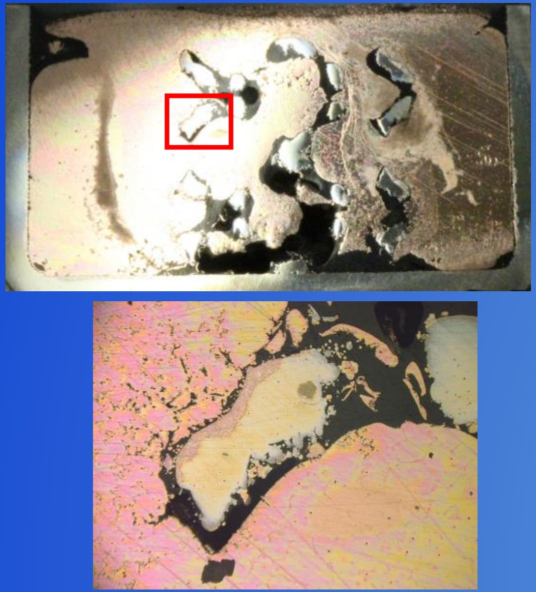
Dode M - 13%RD - 5 mm

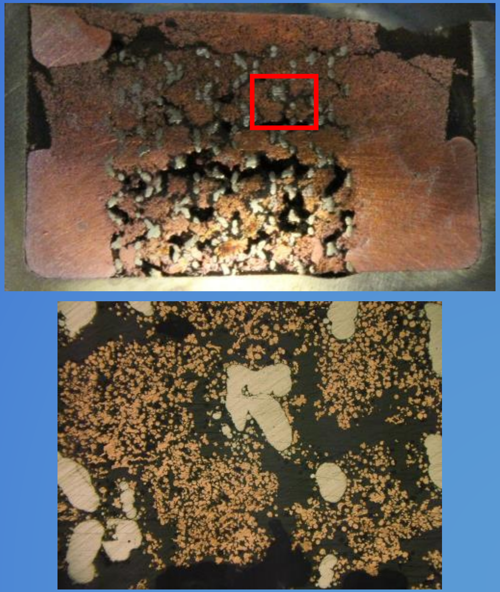
Dode M - 13%RD - 2 mm

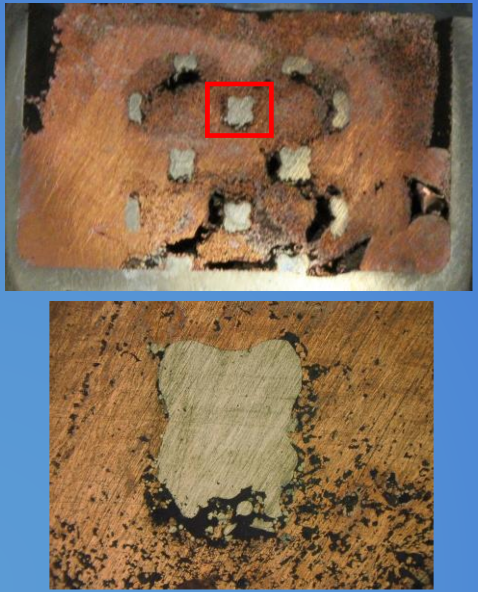
Rhombic Dodecahedron - 20%RD - 5 mm

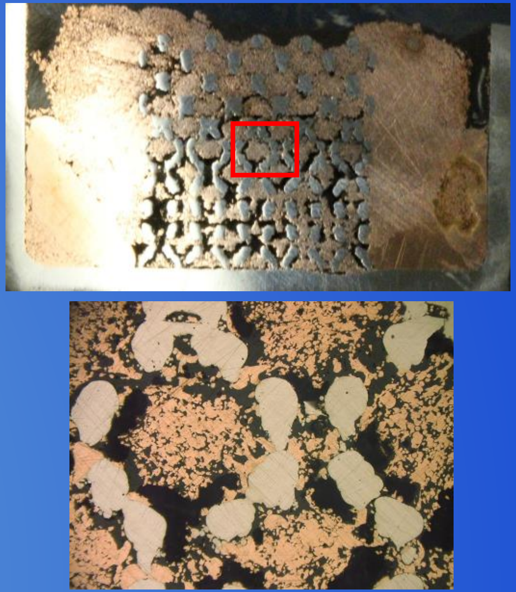
Rhombic Dodecahedron - 20%RD - 2 mm


Diamond - 20%RD - 5 mm

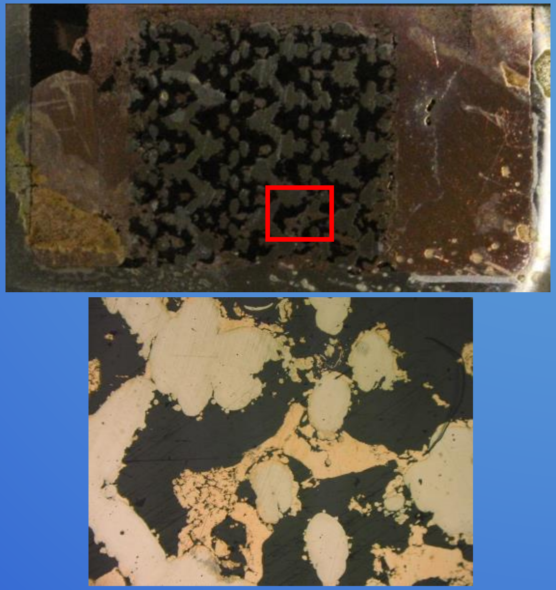
Diamond - 20%RD - 2 mm

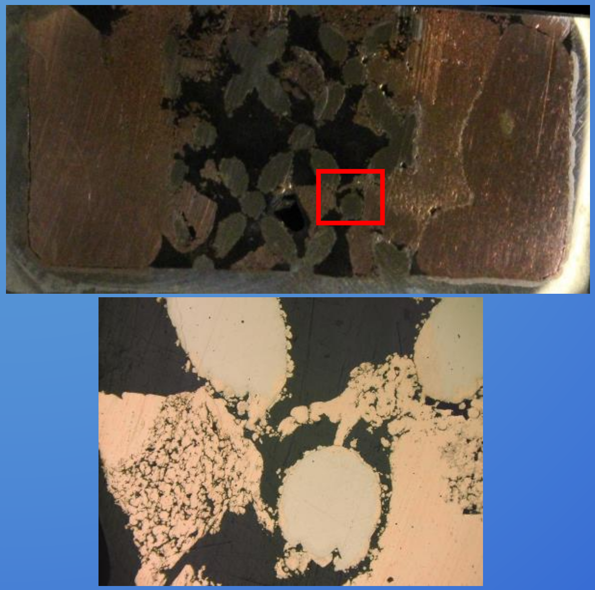
Octet Truss - 30%RD - 5 mm

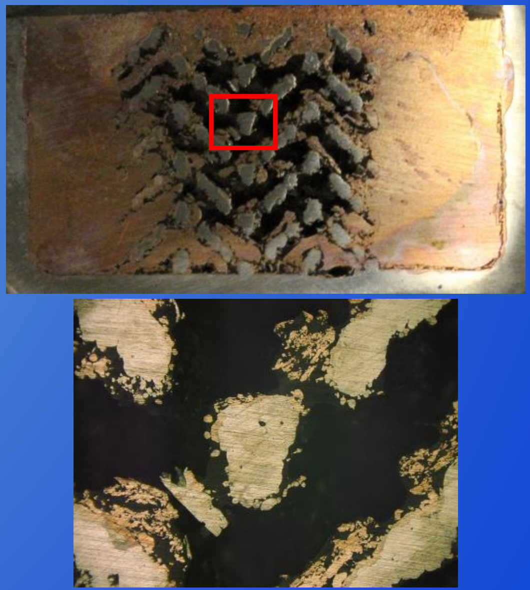
Octet Truss - 30%RD - 2 mm

Conclusions

- Mechanical properties primarily influenced %RD, secondarily by lattice topology, and finally by unit cell size.
- Coarse unit cell structures exhibit significantly greater elongation before failure compared to fine unit cells due to thicker strut sizes.
- Thermal conductivity proportional to %RD and not necessarily to lattice topology or unit cell size.
- Flow coefficient proportional to unit cell size: fine unit cells have more struts per unit volume and therefore higher flow losses.
- Convective heat transfer coefficient inversely proportional to unit cell size: fine unit cells have more surface area per unit volume.
- Infiltration density proportional with unit cell size and topology open cell volume.

Recommendations for Future Work

- Functional gradient and topology optimized structures generated with Autodesk Netfabb.
- Repeat characterization on optimized topologies.
- Independent evaluation of topologies with FEA tools.
- Compare mechanical test to simulation predictions.
- Centrifugal casting or HIP to aid in near-fully dense infiltration.
- Ultra-fine lattice structure with customized parameters.

Acknowledgments

- The author would like to acknowledge Majid Babai, Susan Barber, Catherine Bell, Mark Black, Hoss Burtts, Daniel Cavender, Jeffrey Clounch, Kenneth Cooper, Zachary Jones, Ron Lee, James Lydon, Samantha McLeroy, Pat Salvail, Ellen Rabenburg, Summer Roden, Omar Rodriguez, Jason Turpin, and Brian West of NASA MSFC; Jonaaron Jones and Devon Burkle of Volunteer Aerospace Inc.

- The opinions expressed in this presentation are those of the author and do not necessary reflect the views of NASA or any NASA Project.


PROPULSION
ER
NASA
NASA MSFC
EM
Materials & Processes Lab